# Bayesian optimization of single-atom alloys and other bimetallics:

# Efficient screening for alkane transformations, $CO_2$ reduction and hydrogen evolution

Gbolade O. Kayode,[a] Avery Hill,[a] and Matthew M. Montemore.[a]

[a] Department of Chemical and Biomolecular Engineering, Tulane University, New Orleans, LA 70118, USA

**S1.** Search campaign across methane-intermediate dataset.

Initial set of calculations: Y, Cr, Tl, Pt, Cu, W, In, Al

Search space: Sc, Ti, V, Mn, Fe, Co, Ni, Zn, Ga, Zr, Nb, Mo, Tc, Ru, Rh, Pd, Ag, Cd, Sn, Hf, Ta, Re, Os, Ir, Au, Pb

**S2.** Search campaign across H dataset.

Initial set of calculations: Cr, Pt, Cu, W, Mo, Pd (for Ag & Au based SAAs)

Initial set of calculations: Cr, Pt, W, Mo, Pd (for Cu based SAAs)

Search space for Ag: Au, Co, Fe, Hf, Ir, Mn, Ni, Re, Rh, Ru, Sc, Ta, Tc, Ti, V, Zn.

Search space for Au: Co, Fe, Hf, Ir, Mn, Ni, Re, Rh, Ru, Sc, Ta, Tc, Ti, V, Zn

Search space for Cu: Au, Co, Fe, Hf, Ir, Mn, Ni, Re, Rh, Ru, Sc, Ta, Tc, Ti, V, Zn

**S3.** Search campaign for $CO_2$ reduction.

Initial set of calculations: $Pd_1Ag$, $Ni_1Ag$, $Cr_1Ag$, $Cu_1Ag$, $Hf_1Ag$, $Mn_1Ag$, $Sc_1Ag$, $Ti_1Ag$, $Pd_1Au$, $Hf_1Au$, $Sc_1Au$, $Ti_1Au$, $Ti_1Cu$, $Ru_1Cu$, $Ir_1Cu$, $Co_1Cu$, $Rh_1Cu$, $Fe_1Cu$, $Ni_1Cu$, $Pt_1Cu$, $Mn_1Cu$, $Pd_1Cu$.

Search space: $Ti_1Ag$, $V_1Ag$, $Fe_1Ag$, $Co_1Ag$, $Zn_1Ag$, $Y_1Ag$, $Zr_1Ag$, $Nb_1Ag$, $Mo_1Ag$, $Tc_1Ag$, $Ru_1Ag$, $Rh_1Ag$, $Cd_1Ag$, $Ta_1Ag$, $W_1Ag$, $Re_1Ag$, $Os_1Ag$, $Ir_1Ag$, $Pt_1Ag$, $Au_1Ag$, $Ga_1Ag$, $In_1Ag$, $Tl_1Ag$, $Pb_1Ag$, $Bi_1Ag$, $V_1Au$, $Cr_1Au$, $Mn_1Au$, $Fe_1Au$, $Co_1Au$, $Ni_1Au$, $Cu_1Au$, $Zn_1Au$, $Y_1Au$, $Zr_1Au$, $Nb_1Au$, $Mo_1Au$, $Tc_1Au$, $Ru_1Au$, $Rh_1Au$, $Ag_1Au$, $Cd_1Au$, $Ta_1Au$, $W_1Au$, $Re_1Au$, $Os_1Au$, $Ir_1Au$, $Pt_1Au$,

$Ga_1Au$, $In_1Au$, $Tl_1Au$, $Pb_1Au$, $Bi_1Au$, $Sc_1Cu$, $V_1Cu$, $Cr_1Cu$, $Zn_1Cu$, $Y_1Cu$, $Zr_1Cu$, $Nb_1Cu$, $Mo_1Cu$, $Tc_1Cu$, $Ag_1Cu$, $Cd_1Cu$, $Hf_1Cu$, $Ta_1Cu$, $W_1Cu$, $Re_1Cu$, $Os_1Cu$, $Au_1Cu$, $Ga_1Cu$, $In_1Cu$, $Tl_1Cu$, $Pb_1Cu$, $Bi_1Cu$.

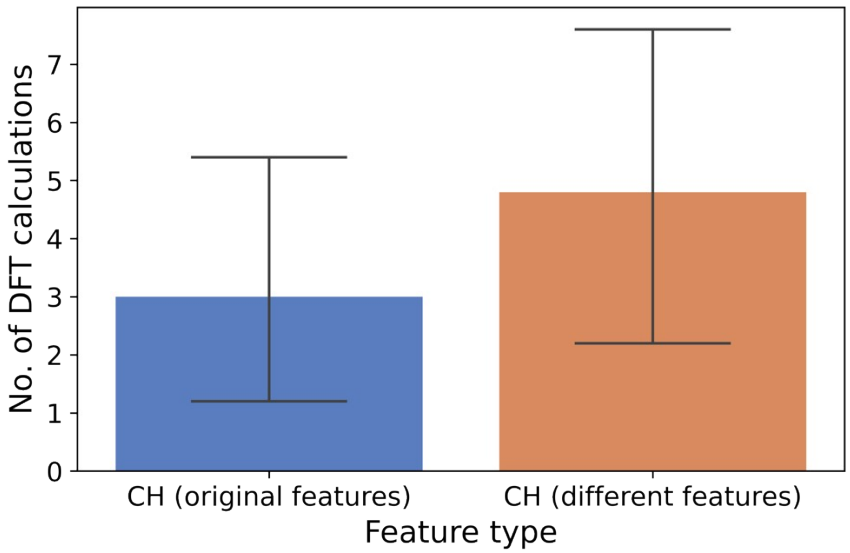


**Figure S1**: 5-fold BO search campaign using our original feature set and an entirely new feature set. This new feature set comprised the heat of formation of the dopant metal, dipole polarizability of the dopant metal, Pauling electronegativity of the dopant metal, fusion heat of the dopant metal. The BO workflow is still reasonably efficient even using new feature set.

## **S4.** Single-atom alloy stability tests

To evaluate the stability of SAAs, two key aspects need to be considered: dopant aggregation and dopant segregation. Dopant aggregation must be prevented for the dopant to remain dispersed as single atoms rather than forming clusters or islands. On the other hand, dopant segregation into the subsurface or bulk of the material would prevent it from directly interacting with reacting species. Dopant aggregation has generally been found to be a more important test, because adsorbates—which are generally present under reaction conditions—often stabilize dopants in the surface layer.

As a simple criterion for the formation of thermodynamically stable SAAs rather than clusters or islands (i.e., to prevent dopant aggregation), the reaction energy $2D_1M_{35} \rightarrow D_2M_{34} + M_{36}$ should be positive.[1–4] $D_1M_{35}$ represents the SAA with dopant *D* and host *M*, $D_2M_{34}$ is a dopant dimer, and $M_{36}$ is a pure surface of the host metal. For dopant segregation, the difference in energy between the dopant in the subsurface/bulk of the material and the dopant on the surface of the material must be positive. As this is often highly sensitive to adsorbates, this test is often performed with a representative adsorbate on the surface. For example, when considering CO, the energy difference $\Delta E^{CO} = E_{bulk}^{CO} - E_{surface}^{CO}$ must be positive for the dopant to be stabilized at the surface, where $E_{surface}^{CO}$ is the total energy of the case with the dopant in the surface layer and adsorbed CO, while $E_{bulk}^{CO}$ is the total energy of the case with the dopant in the subsurface layer and adsorbed CO.[4,5]

References:


1 K. K. Rao, Q. K. Do, K. Pham, D. Maiti and L. C. Grabow, *Top. Catal.*, 2020, **63**, 728–741.

2 M. T. Darby, R. Réocreux, E. C. H. Sykes, A. Michaelides and M. Stamatakis, *ACS Catal.*, 2018, **8**, 5038–5050.

3 J. Mao, J. Yin, J. Pei, D. Wang and Y. Li, *Nano Today*, 2020, **34**, 100917.

4 R. Réocreux and M. Stamatakis, *Acc. Chem. Res*, 2023, **2022**, 30.

5 K. K. Rao, Q. K. Do, K. Pham, D. Maiti and L. C. Grabow, *Top. Catal.*, 2020, **63**, 728–741.